NON-CONTACT ULTRASONIC CHARACTERISATION OF ANGLED SURFACE DEFECTS

R.S. Edwards, B. Dutton, M.H. Rosli and A.R. Clough

University of Warwick, Department of Physics, Coventry CV4 7AL, U.K.

ABSTRACT. Surface ultrasonic waves have been shown to have many uses in non-destructive testing, in particular for gauging the depth of surface defects. Much of the previous work has assumed that these defects are oriented normal to the surface. However, this is not always the case; for example, rolling contact fatigue in rails propagates at an angle of around 25º to the surface, and this angle may affect the characterisation. We present results using non-contact ultrasonic methods to generate and detect ultrasound on samples with a range of defect angles, and compare these with finite element method (FEM) models. We use both electromagnetic acoustic transducers (EMATs) and laser ultrasound. The depth calibration when measuring ultrasound transmission is considered, and what affect the angle of a defect has. Several other methods of characterising crack depth and angle are also discussed, including the arrival times of reflected and mode-converted waves, the delay in the transmission of the high-frequency Rayleigh wave, and the enhancement of the signal at the defect in both the in-plane and out-of-plane components.

Keywords: EMAT, laser ultrasound, defect characterization, Rayleigh wave
PACS: 43.35.Yb, 43.38.Dv, 43.60.+d, 43.20.Gp, 81.70.Cv

INTRODUCTION

We present investigations of the response of ultrasonic Rayleigh waves to surface defects, and their use in calibrating both the depth and angle to the surface of the defect. It is important to be able to correctly characterise cracking in metals, and Rayleigh waves are known to be useful for gauging the depth of surface defects [1-3], which can be a problem in many industries. Surface waves will interact with surface-breaking cracks, giving a reflected and a transmitted signal which can both potentially be used for characterisation. For a realistic defect with rough edges, the reflected wave may be scattered and hence the reflected signal received at a far-field detection point may be small, and transmitted signals may be more appropriate for characterisation.

We have shown previously that surface defects will act like filters to a broadband incident Rayleigh wave; a proportion of the wave will be reflected and a proportion transmitted, with the amplitude dependent on the crack depth, and the transmitted wave amplitude dropping off approximately exponentially with depth [1]. By exploiting both the filtering action of the crack and the broadband nature of several non-contact ultrasonic techniques, it is possible to use the frequency content of the transmitted waves to measure a cut-off frequency, which can again be used to gauge the depth [1]. This has applications for many measurements, including high speed rail testing [3].

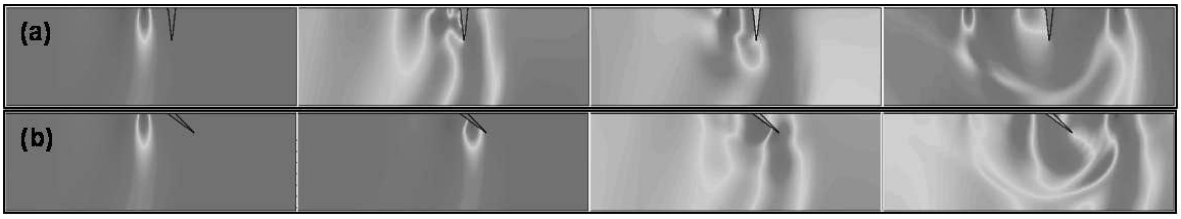

FIGURE 1. (a) Rayleigh wave propagation for a surface-normal defect, at different times. (b) The same, but for a defect inclined at 140º to the surface. Note that the colour scale is rescaled for each image.

In the near-field, enhancement of the Rayleigh wave signal amplitude has been reported by several groups [4-8]. At a surface defect inclined normal to the surface the incident and reflected Rayleigh waves will interfere. Further interference occurs between these waves and those mode converted from the incident Rayleigh wave, such as the surface-skimming longitudinal wave. At the detection position where this interference is constructive an increased signal is measured [4]. Similar enhancement has also been observed when using laser generation close to defects. In this case, the mode converted waves are significantly attenuated before reaching the detection point and have only a small effect. However, there are extra enhancements due to truncation of the laser source over a defect and the change in boundary conditions [5,6], and the technique has been reported as the scanning laser line source (SLLS) technique with applications to pinpointing the position of a defect [6-8]. When defects are partially closed it has been shown that the signal can be further enhanced at certain frequencies as the sides 'clap' together [6,8].

The majority of this previous work has assumed that a slot machined normal to the sample surface is a suitable approximation to a surface defect. In many cases this is applicable, however, not all defects grow in this direction. As an example, rolling contact fatigue in rails grows initially at around 25º to the sample surface, and it is to be expected that this will have some affect on the results. Kinra and Vu performed initial studies of the effect of crack angle using narrowband waves [9]. Several groups have produced models of waves incident on wedge-shaped samples, looking at the reflection from the wedge point and the waves transmitted around the tip, but there has not, to the best of our knowledge, been a modelled study of the effect of finite depth angled cracks [10,11].

Figure 1 shows images taken from a finite element method (FEM) model of two different defects. This shows the difference in the reflected and transmitted waves for two cracks, one inclined at 90º to the surface, and the other at 140º. It is clear from these images that an investigation into the effect of crack angle is warranted, and that we would expect some variation in the reflected and transmitted waves with angle [12]. Here, we consider various non-contact ultrasonic techniques, including electromagnetic acoustic transducers (EMATs) and scanning laser generation and detection, and identify potential methods for characterisation of both depth and angle of surface defects.

EXPERIMENT AND MODEL DETAILS

This work considers a combination of experiments and modelling of laser generation and detection, and EMAT techniques. The measurement configuration is shown in figure 2(a); the generation and detection points are at separate positions on the sample, with the detection, or both generation and detection, scanned along the sample. A set of aluminium samples have been produced with defects inclined at an angle θ to the sample surface and a variety of depths, with either the crack length or the vertical depth (measured from the sample surface directly down to the crack tip) held constant for measurements.

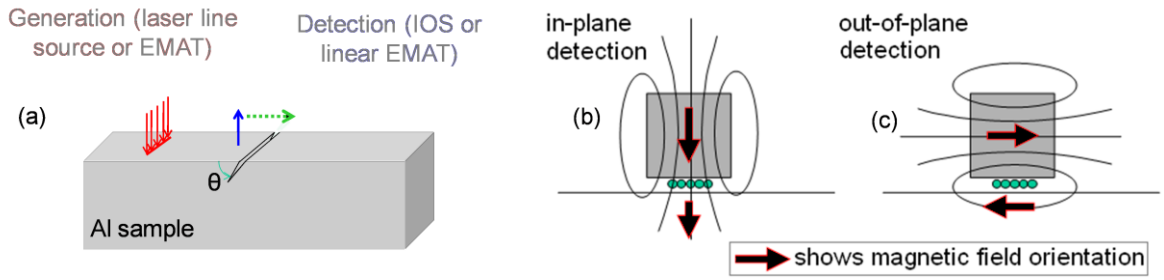

FIGURE 2. (a) Experimental set-up. The generation and/or detection point (laser or EMAT) are scanned over a defect, which is inclined at an angle θ to the sample surface. (b) and (c) show the magnet and linear coil configuration for detection EMATs primarily sensitive to in-plane or out-of-plane velocities.

A pulsed Nd:YAG generation laser was used for laser generation (1064 nm wavelength, 10 ns pulse duration) focussed into a line of approximately 6 mm by 300 µm, oriented parallel to the defect. The laser was used in the thermoelastic regime and generated a broadband Rayleigh wave with a centre frequency of 1.67 MHz. Laser detection used an IOS two-wave mixer interferometer with a detection point of 200 µm diameter, sensitive to out-of-plane displacements and able to measure signals on rough samples [13]. Laser measurements were modelled using PZFlex FEM software. The generation pulse was approximated as a loading force of 10 ns duration with appropriate boundary conditions. More details are available in [14,15].

For the EMAT measurements a linear generation coil was used, with more details about the use of this type of EMAT available in references [1,16]. This linear coil generated a broadband pulse with a central frequency of 200 kHz. For detection a linear coil wrapped around a permanent magnet was also used. Through consideration of the coil configuration and magnetic field orientation it is possible to measure primarily the in-plane or out-of-plane velocity component of **v;** the Lorentz force **F** is given by,

$$\mathbf{F} = q\mathbf{v} \times \mathbf{B} \qquad (1)$$

where **B** is the magnetic field from the permanent magnet. For a linear coil, a field oriented into the sample will give a detection EMAT primarily sensitive to in-plane velocity, whereas a field oriented parallel to the sample will give an EMAT primarily sensitive to out-of-plane velocity [17].

EXPERIMENTAL RESULTS

Signal transmission

Previously we have reported the change in the velocity transmission coefficient with defect depth using in-plane sensitive EMATs for 90º defects only, where an approximately exponential decay with defect depth was observed. However, it is to be expected that there is also an angle dependence to the transmission coefficient. Here, EMATs are used to investigate the transmission coefficient for cracks with different vertical depths and angles to the surface. Figure 3(a) shows the results for machined slots inclined at 90º to the surface (solid line), and for 45º and 135º (dashed lines). The transmission coefficient is measurably lower for the 90º defect than for the angled defects. Figure 3(b) shows the transmission for defects with a fixed vertical depth of 5 mm inclined at different angles to the sample surface; again, an angle dependence is observed. Hence, in order to correctly gauge the depth of a defect, some knowledge of the angle must also be obtained.

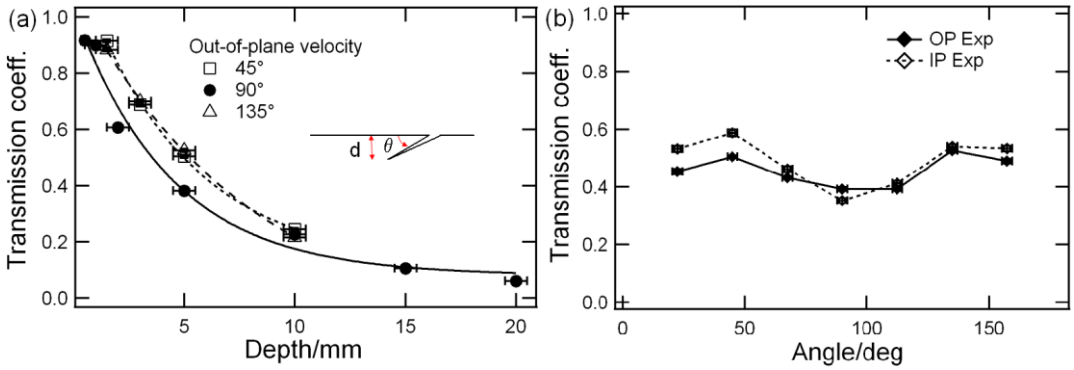

FIGURE 3. (a) shows the approximately exponential drop in transmission for 135º, 90º and 45º defects, as a function of depth, for out-of-plane EMAT measurements. Here, the vertical depth is varied. (b) shows the out-of-plane (solid line) and in-plane (dotted line) transmission for a 5 mm deep defect.

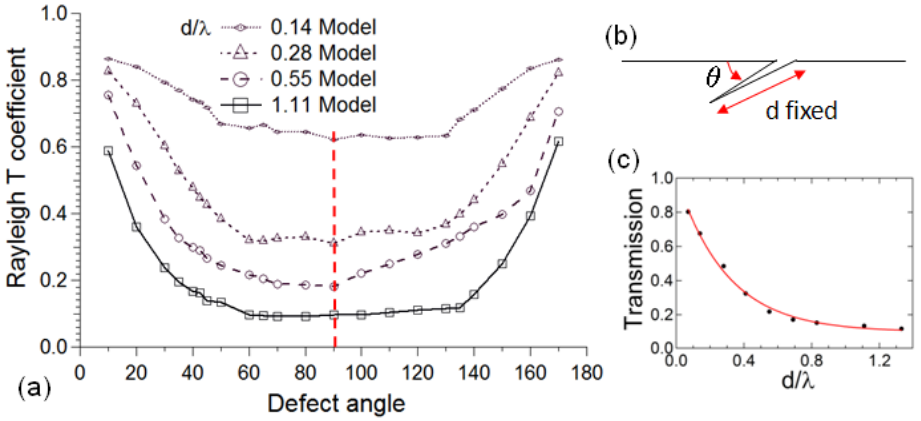

FIGURE 4. Transmission coefficient for Rayleigh wave displacement, for (a) different angles and (b) defect depths at 90º. At each angle, the drop-off with defect depth is approximately exponential.

For laser measurements the higher spatial resolution enables work at higher frequencies, and a larger range of angles and depths were investigated through combination with modelling. Figure 4 shows transmission measurements as a function of angle for several different defect depths (normalised to the central wavelength of the Rayleigh wave). For these measurements the length of the defect, rather than its vertical depth, was held fixed while the angle was varied. Comparison with the variation of the EMAT results with angle (figure 3(b)) shows that the dominant factor affecting the transmitted wave amplitude is the vertical depth.

Figure 4(c) shows the approximately exponential decay of the transmission with depth for a 90º defect. One can consider variation of the transmission T to lie along the line;

$$T \approx \exp\left[-d \sin\theta / (\lambda\tau)\right] \qquad (2)$$

where d is the crack length, θ is the angle relative to the sample surface, λ is the central wavelength of the Rayleigh wave and τ is a fitting parameter [1]. Fits of the data confirm that the angle dependence in figure 4(a) is mainly due to variation in the vertical depth of the cracks as the angle is changed, however, there is still some other angle dependence, as observed in figure 3(b).

Wave arrival times

These results confirm that there is angle dependence to the transmitted amplitude of the Rayleigh wave, and hence, to obtain a correct characterisation, one also requires knowledge of the defect orientation. We turn now to other features which are dependent on the crack properties. Figure 5 shows B-scans produced from models of the laser generation

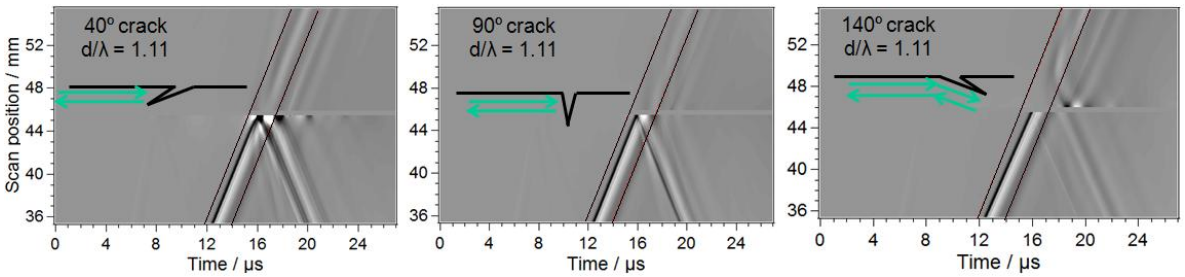

FIGURE 5. B-scans generated for cracks of different angles. In each case, peak to peak signal analysis considers the Rayleigh wave whose arrival time is within the window shown by the dashed lines.

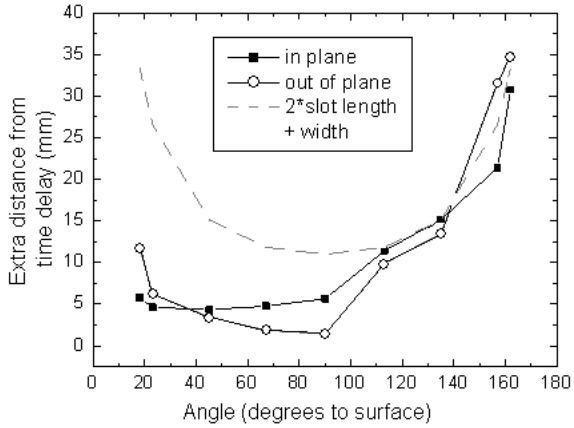

FIGURE 6. Extra distance travelled for each wave, calculated from the time delay of the transmitted Rayleigh wave from EMAT measurements.

and detection measurements, showing the arrival times of the out-of-plane component of the waves as the separation between generation and detection points is increased. The Rayleigh wave arrival time is windowed by the dashed lines, and for larger angles a delay in the arrival of the transmitted Rayleigh wave is observed in the near-field.

EMAT measurements also show a dependence of the delay time on crack angle. Figure 6 shows analysis of this arrival time for a set of defects, each of vertical depth 5 mm. The arrival time is converted into the extra distance travelled by the wave during transmission, for both in-plane and out-of-plane velocity measurements. For angles less than 90º the delay remains similar, while for angles greater than 90º the distance the waves travel increases, consistent with the wave behaviour in the model images shown in figure 1; the sum of the lengths of both crack faces is shown as a dashed line.

Another feature clear on the B-scans presented in figure 5 is the angle dependence of the wave arrival times, and these can be calculated and used to identify each wavemode. Waves which remain as surface waves (i.e. Rayleigh waves or those mode converted to surface skimming longitudinal waves) will have a dependence only on the separation of the generation and detection points, the distance to the crack and the crack length. However, waves which have been mode converted at the crack to bulk waves have arrival times dependent on both crack length and angle. This is covered in more detail in [14] and also in [15], within these proceedings, where figures show the agreement between B-scans and calculated arrival times.

Signal enhancement

Another effect which can be considered is the signal enhancement observed when either the generation or detection point reaches the defect [4-8]. Reference [15], also in these proceedings, details the difference in enhancements when comparing scanning the

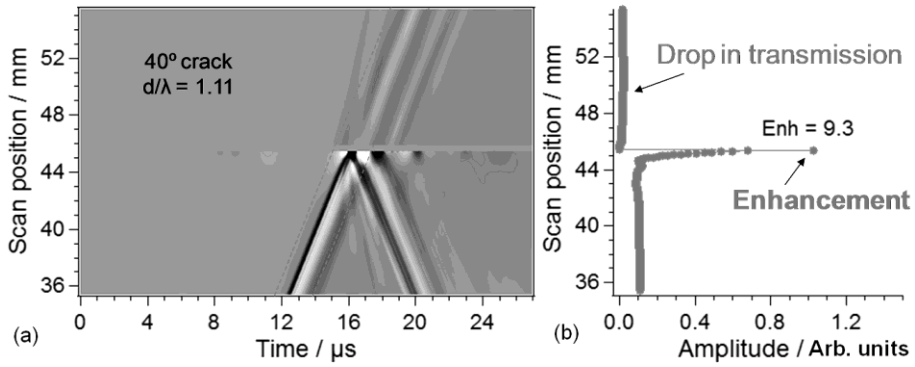

FIGURE 7. Measurement of the peak to peak amplitude of the Rayleigh wave in (a) gives the plot in (b); the drop in transmission and signal enhancement are clear.

laser generation or detection point over the defect. Here we consider primarily the difference between the enhancement of the in-plane and out-of-plane signals. Figure 7 shows again the B-scan for the modelled out-of-plane displacement for a 40º crack. The peak-to-peak amplitude of the windowed Rayleigh wave is calculated and plotted in (b). The drop in transmission when the crack blocks signals is clear, however, we also observe an enhanced signal when the detection point is very close to the crack [4,15], explained in more detail in [15].

The use of EMATs allows one to consider primarily either in-plane or out-of-plane signals. As shown in [4], for a 90º smooth defect it is expected that the in-plane enhancement is larger than the out-of-plane. This is due to the constructive interference of the incident and reflected Rayleigh waves with a mode-converted surface skimming longitudinal wave, which has a significant component in the in-plane but little motion in the out-of-plane. Figure 8 shows the measured enhancements using different detection EMATs for cracks with a fixed vertical depth of 5 mm; enhancements show significant angle dependence, and for cracks with angles of less than approximately 45º the out-of-plane component dominates. As the vertical depth is held constant the proportion of low-frequency waves able to pass underneath the defect remains constant. However, as the defect angle becomes shallower, the waves incident on the crack opening travel along a wedge. This will have some affect on the mode-conversion of the waves, and the increase in enhancement for shallow angles is being investigated.

Finally, one can also consider the frequency enhancements [6,8]. It has been observed that, on scanning a sample, the central frequency of the windowed Rayleigh wave shifts on approaching the defect, and this can be used for characterisation and/or identification of a surface-breaking defect [6-8]. The magnitude of the central frequency

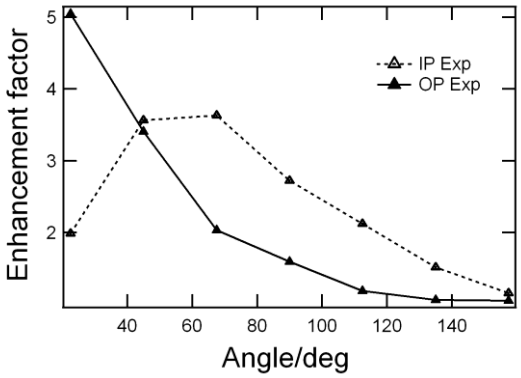

FIGURE 8. In-plane (dashed) and out-of-plane (solid line) enhancements from EMAT measurements, plotted as a function of defect angle for a fixed vertical depth of 5 mm.

will closely follow the amplitude measurements. However, one can also consider the high-frequency enhancement observed at frequencies which were not present at significant amplitudes in the original pulse [6,8]. For shallow angles, there is again a significant enhancement measured at higher frequencies, and windowing the magnitude of the signal at a frequency of 3.5 MHz shows significant promise for pinpointing the presence of a defect.

CONCLUSIONS AND FUTURE WORK

We have shown that it is essential to consider both the crack depth and angle relative to the surface when correctly characterising a defect; previous calibrations considering only defects normal to the surface show the correct trend but may not accurately gauge the depth of an unknown defect. However, there are several effects which can be considered when analysing data. Firstly, the appearance of the B-scan can be considered. In [18] we discussed image analysis, using the oscillating enhancement patterns observed for defects with angles less than approximately 70º, or greater than approximately 110º, to identify using genetic algorithms whether a defect is angled or normal. We can also consider the delay of the Rayleigh wave, which has both crack length and angle dependence, and the arrival times of the Rayleigh and mode converted waves, which can be fitted to the expected times for a given depth and angle [15]. Finally, we can consider the enhancement of the signals, and in particular when performing EMAT measurements, it may be possible to compare in-plane and out-of-plane enhancements. By combining all of these measurements it will be possible to identify the angle range and hence decide a suitable depth calibration curve to use, and a suitable algorithm for consideration of all of these effects is currently under development.

The next stage of the project will investigate the effect of more realistic defects, for example those which are rough or partially closed, and more complicated crack geometries, such as branched defects.

ACKNOWLEDGEMENTS

This work was funded by the European Research Council under grant 202735, ERC Starting Independent Researcher Grant.

REFERENCES

1. Edwards, R.S., S. Dixon, and X. Jian, *Ultrasonics* **44** (1) 93 (2006)
2. I.A. Viktorov. “Rayleigh and Lamb waves: physical theory and applications.” *Plenum Press* 1967
3. Edwards, R.S., Dixon S., and Jian X., *NDT & E International* **39** (6) 468 (2006)
4. Edwards, R.S., Jian X. and Dixon S.., *Applied Physics Letters* **87** (19) 3 (2005)
5. C.B. Scruby, L.E. Drain. “Laser ultrasonics: techniques and applications.” *Adam Hilger*, 1990
6. Dixon S., Cann B., Carroll D.L., Fan Y. and Edwards R.S., *Nondestructive Testing and Evaluation* **23** (1) 25 (2008)
7. Kromine A.K., Fomitchov P.A., Krishnaswamy S. and Achenbach J.D., *Materials Evaluation* **58** (2) 173 (2000)
8. Arias I. and Achenbach J.D., *Wave Motion* **39** (1) 61 (2004)

9. Kinra V.K. and Vu B.Q., *Journal of the Acoustical Society of America* **79** (6) 1688 (1986)
10. Babich V.M., Borovikov V.A., Fradkin L.J., Kamotski V. and Samok-ish B.A., *NDT & E International* **37** (2) 105 (2004)
11. Fujii K., *Bulletin of the Seismological Society of America* **84** (6) 1916 (1994)
12. DuttonB., Rosli M.H. and Edwards R.S., *Review of Progress in QNDE* **29** 647 (2010)
13. Klien M., Bacher G., Grunnet-Jepson A., Wright D. and Moerner W., *Optics communications* 162 79 – 84 (1999)
14. Dutton B., Clough A.R., Rosli M.H. and Edwards R.S., *under review*
15. Clough A.R., Dutton B. and Edwards R.S., *these proceedings*
16. Frost H.M., *Physical Acoustics* **14** 179 (1979)
17. Edwards R.S., Dixon S., Fan Y. and Jian X., *Review of Progress in QNDE* **27** 841 (2007)
18. Rosli M.H., Edwards R.S., Dutton B., Johnson C.G. and Cattani P., *Review of Progress in QNDE* **29** 1593 (2010)